Journal of Computer-Aided Molecular Design, **12:** 361–372, 1998.
KLUWER/ESCOM

Toward the identification of the cardiac cGMP inhibited-phosphodiesterase catalytic site

Paola Fossa[a,*], Raffaella Boggia[b] & Luisa Mosti[a]
[a]*Dipartimento di Scienze Farmaceutiche, Università degli Studi di Genova, Viale Benedetto XV 3, I-16132 Genova, Italy;* [b]*Dipartimento di Chimica e Tecnologia Farmaceutiche ed Alimentari, Università degli Studi di Genova, Via Brigata Salerno (ponte), I-16147 Genova, Italy*

Received 10 March 1997; Accepted 17 December 1997

Key words: 3D-SAR, molecular modelling, phosphodiesterase inhibitors, pharmacophoric model

Summary

Cyclic nucleotide phosphodiesterases (PDEs) comprise a complex group of enzymes; five major PDE families or classes with distinctive properties have been identified. Among these a great deal of interest has recently been focused on the so called cGMP-inhibited low K_m cAMP phosphodiesterase (cGI PDE) or PDE III. A number of positive inotropic agents, including the well-known milrinone, display a specific inhibition of PDE III as primary mechanism of action. Recent studies have been carried out to develop a pharmacophore model of the PDE III active site. We therefore performed molecular modelling and 3D-SAR studies so as to better define structural requirements for potent and selective enzymatic inhibition. The DISCO (DIStance COmparison) strategy has been applied on a set of compounds taken from literature and a milrinone analogue previously synthesized by us, all of which are characterized by a marked inotropic effect but with varying degrees of enzyme selectivity. A common pharmacophoric model was derived, validated and considered as starting point to perform a 3D-SAR study using the GRID force field and PCA (Principal Component Analysis) with the aim of rationally designing more selective inhibitors. This paper presents the results of this theoretical approach.

Introduction

Congestive heart failure (CHF) is a chronic and ultimately fatal disease whose pharmacological treatment encompasses several classes of drugs. Primary inotropic agents include steroidal derivatives such as cardiac glycosides, but their narrow therapeutic index has stimulated an intensive search for alternatives. This search has resulted in the discovery of adrenergic agonists such as dobutamine and more recently bipyridine derivatives such as milrinone [1].

The favourable therapeutic properties of this latter class of agents have encouraged the synthesis of numerous cardiotonics characterized by diverse heterocyclic nuclei which have received considerable attention in the last decade.

Some of these compounds are shown in Figure 1. The primary mechanism of action of drugs **1–11** is the specific inhibition of myocardial cGMP-PDE (cyclic GMP-inhibited phosphodiesterase), designated PDE III [2].

Previous extensive and complementary studies proposed a pharmacophoric model for the PDE III catalytic site based on SAR, computational chemistry and molecular graphics [3–6]. It is generally agreed that high affinity PDE III inhibitors should adopt an energetically favoured planar conformation that mimics the anti conformation of cyclic AMP, the natural substrate of the enzyme.

Identification of features common to the most selective inhibitors has led to a 'five-point model' with: presence of a strong dipole (carbonyl moiety) at one end of the molecule, an adjacent acid proton, a small sized alkyl substituent on the heterocyclic ring, a relatively flat overall topography and an electron rich

*To whom correspondence should be addressed.

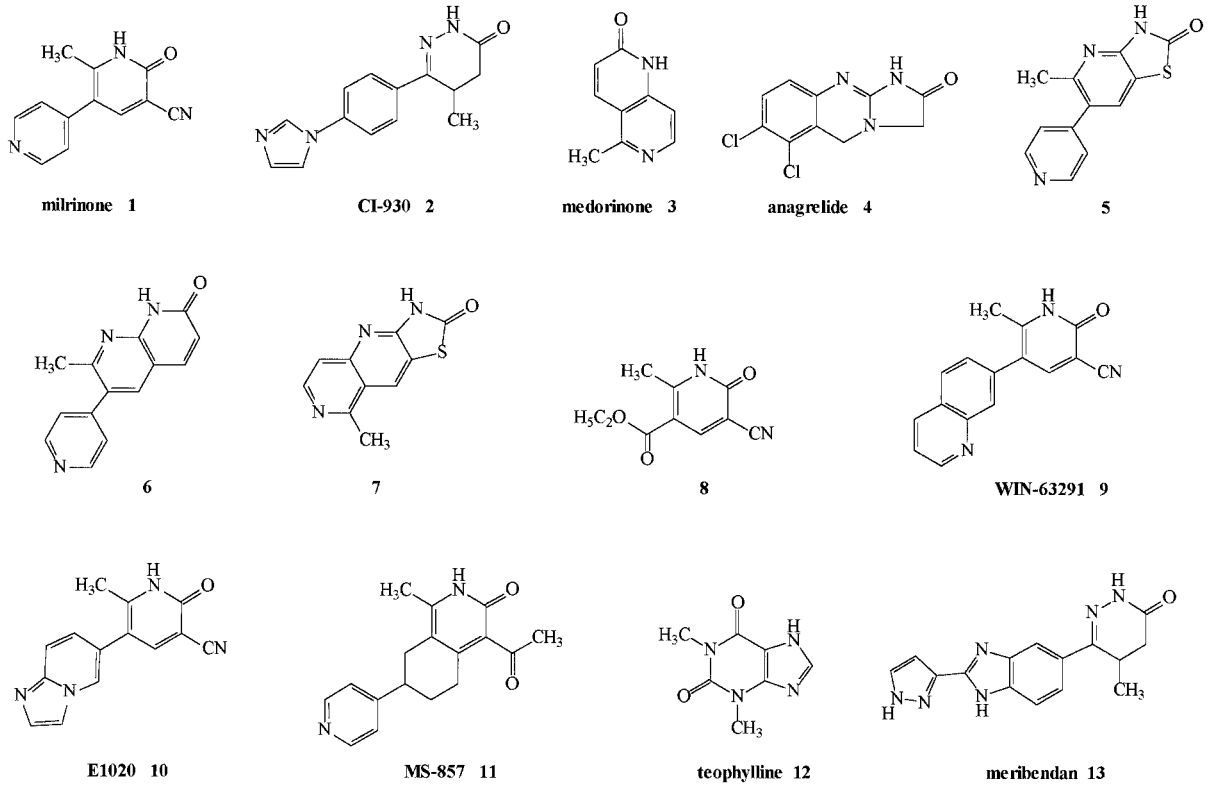

Figure 1. Molecular formulas of some selective (**1–11**, **13**) and non-selective (**12**) PDE III inhibitors.

centre and/or a hydrogen bond acceptor site opposite to the dipole.

Our interest in improving inotropic activity of some pyridonic derivatives already synthesised in our group [7] led us to reconsider the pharmacophoric models previously described and to further investigate the important interactions necessary for high selectivity for the enzyme catalytic site, through an indirect approach.

In the present work, the DISCO (DIStance COmparison) module [8] as implemented in the Sybyl package [9] was employed to generate a new topographical model of the PDE III catalytic site, which accounts for the different selectivity shown by the seven diverse classes of inhibitors taken from literature and by compound **8**, synthesised in our laboratories (Figure 1, Table 1).

DISCO is a useful strategy in defining both a bioactive conformation and a superimposition rule for a set of compounds. DISCO uses a clique-detection method to find superimpositions that contain at least one conformation of each molecule and user-specified numbers of point types. If a clique meets the user-specified set-up criteria (e.g., a minimum number of site points matched, distance tolerances, etc.), a pharmacophoric map is drawn. Any solution includes all conformations that match the superposition rule chosen as reference by DISCO or by the operator. The pharmacophoric points matched by the program are grouped into the following four classes: hydrogen bond donor atoms (DL), hydrogen bond acceptor atoms (AL), charged atom centres (CHG), centres of hydrophobic rings (HY). In addition, sites projected from the ligand hypothesized to exist in the biological receptor are included (Donor Site, DS, and Acceptor Site, AS).

The molecular superimpositions proposed by DISCO have been employed to perform a 3D-SAR study using the GRID force field [10] and the chemometrical technique of Principal Component Analysis (PCA) [11]. The aim of this procedure was to validate DISCO results and to propose a strategy to rationally design new inhibitors. The program GRID calculates the interaction between a small chemical group (probe) and the chemical structures taken into account (targets). GRID is a computational procedure

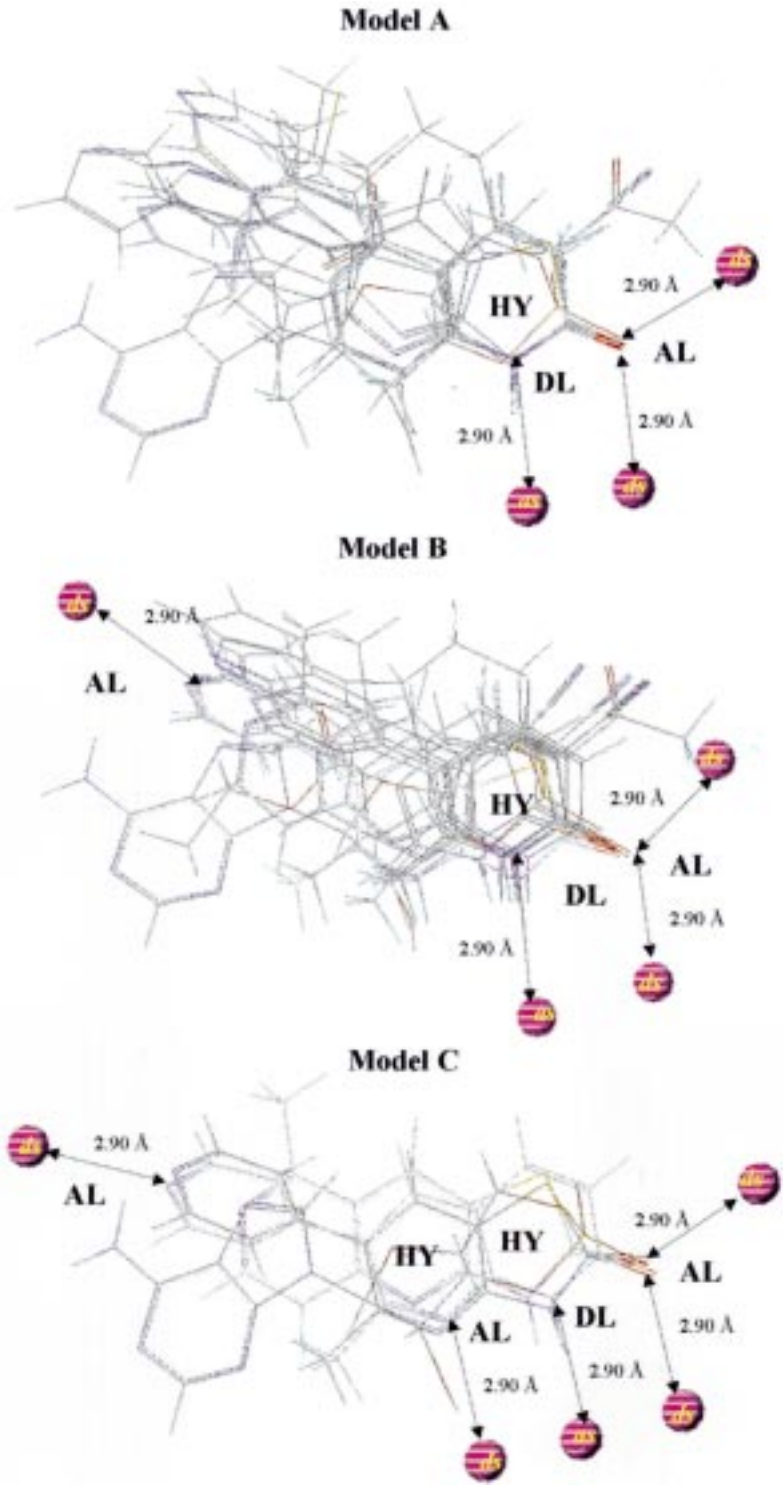

Figure 2. Model A: superimposition of compounds **1–11** and cAMP. Model B: superimposition of compounds **1**, **3**, **5–11** and cAMP. Model C: superimposition of compounds **5–7** and cAMP. The following pharmacophoric points are used: AL, hydrogen bond acceptor atom; DL, hydrogen bond donor atom; HY, centre of hydrophobic ring; *ds*, donor site; *as*, acceptor site.

Table 1. IC_{50} values for compounds **1–13**[a]

Compound	IC_{50} (μM)	Reference number
1	2.50	5
	8.00	[b]
2	0.60	5
3	0.55	22
4	0.10	15
5	0.02	23
6	0.06	23
7	0.06	18
8	10.00	[b]
9	0.10	24
10	0.35	25
11	1.25	25
12	390	20
13	0.03	21

[a] Since no study actually exists in which all of these agents were evaluated on purified PDE III under the same experimental conditions, the values given in this table are taken from a number of different literature sources. Only in case of milrinone **1**, used as reference compound, the published IC_{50} value was confirmed by us. Due to these reasons data have been considered only from a qualitative point of view.

[b] Data not yet published by us.

for detecting energetically favourable binding sites on molecules of known three-dimensional structure using an empirical energy potential which consists of Lennard-Jones, electrostatic and hydrogen-bonding terms. GRID probes are very specific and they may be representative of important chemical groups present in the enzymatic active site. Since GRID calculations yield a very large number of interaction energies between probe and targets, the PCA was used to extract, visualise and rationalise as much of the useful information as possible.

Computational methods

A set of seven structurally diverse classes of compounds showing PDE III inhibitory activity was energy minimised with MacroModel [12, 13] using X-ray data as starting geometries when available or the interactive model building of MacroModel.

Conformational analysis was carried out using the AMBER* force field [14] included in MacroModel. The reliability of the force field was both previously stated in literature [15] and confirmed by experimental data.

Tautomerism for basic nitrogens (**12** and **13**) was taken into account performing conformational analysis. The keto-enol tautomeric equilibrium for the lactam nitrogen was not computationally considered due to recent experimental results obtained by us [16]. These results showed that the 2-pyridone form predominates over the 2-pyridinol form for most of the studied compounds.

For the flexible compounds a systematic search or a random search (using the Monte Carlo method implemented in MacroModel) was performed. Conformations with an energy more than 21 kJ/mol (5 kcal/mol) above absolute energy minimum were discarded.

In the case of cAMP, the natural substrate of the enzyme, the anti conformation was extracted from the Cambridge Crystallographic Database [17] and the resulting structure after energy minimisation (AMBER* force field) was included in the study.

The DISCO module of Sybyl provided diverse solutions among which three different pharmacophoric models were considered.

Two of the DISCO models (Model A and Model B) were taken as initial alignments for a 3D-SAR study using the GRID computational procedure with different probes and the PCA multivariate statistical technique. Due to the limited number of retained compounds of the last DISCO superimposition (Model C), this was not used for the 3D-SAR analysis.

All the calculations were performed on a Silicon Graphics INDIGO 2 workstation.

Results and discussion

The aim of the present study has been the development of a new pharmacophoric model from a diverse set of compounds having different inhibitory activity of PDE III, using the combination of DISCO, GRID and PCA strategies.

Two features are clearly common to all the inhibitors, namely a hydrogen donor and acceptor (secondary amide). In the first DISCO run we asked the program to derive a model which contained a maximum number of site points common to all the molecules in the training set.

DISCO proposed Model A (Figure 2), a six point model (AL, DL, HY, DS, DS, AS) with a tolerance of 1 Å, derived from compounds **1–11** plus cAMP. AL is

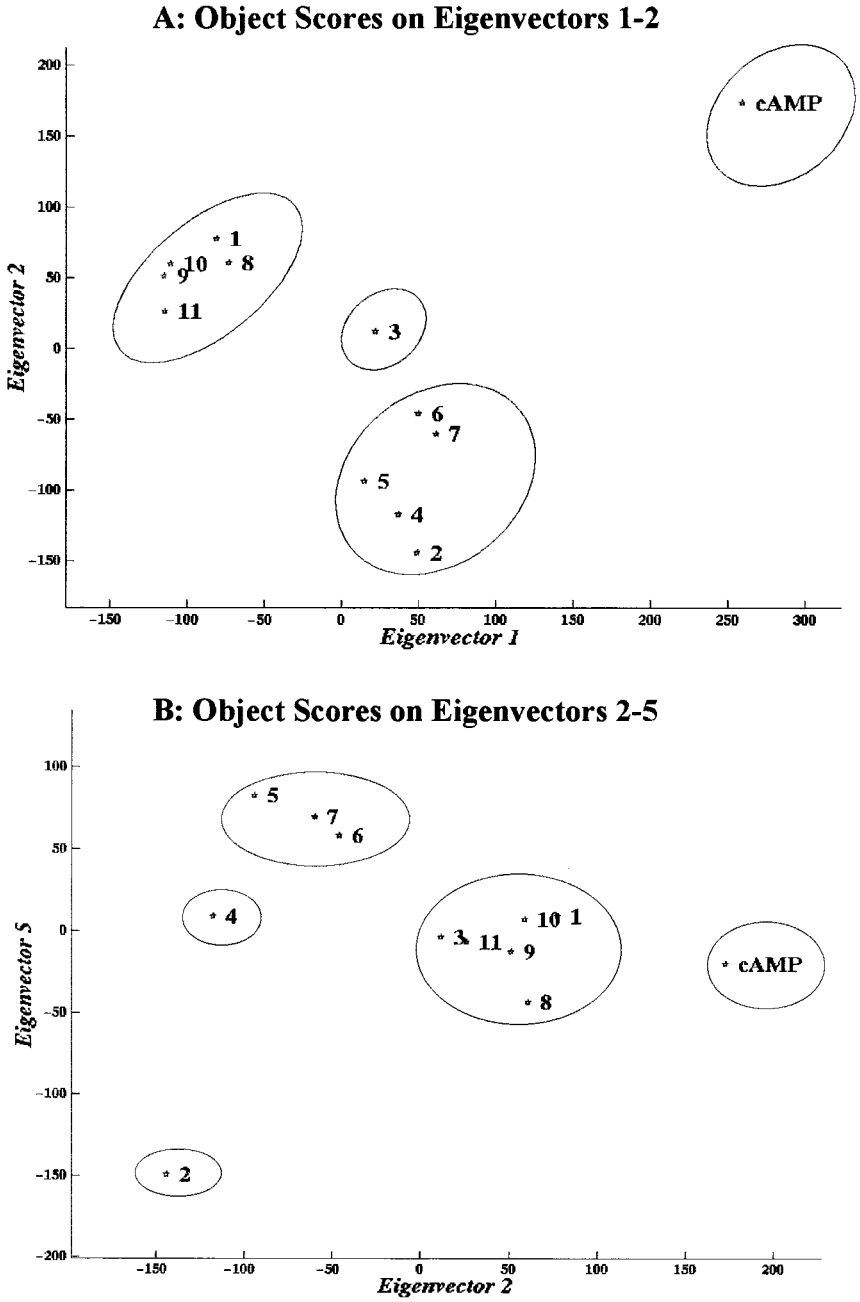

Figure 3. A: Score plot of the first eigenvector vs. the second. This plot shows four separate groups of molecules indicated with circles. B: Score plot of the second eigenvector vs. the fifth. Compounds **2** and **4** are ungrouped from the most selective molecules **5**, **6**, **7** on the fifth eigenvector.

the lactam carbonyl oxygen, DL is the nitrogen of the amide function, HY is the centre of the lactam ring, DS and AS are the putative corresponding points in the biomolecule, derived by extension from the lactamic carbonyl oxygen and nitrogen.

The amide function of the inhibitor molecules is believed to mimic the phosphate group in cAMP and is confirmed as the primary site of binding [5, 6]. Besides, the model points out the location and the characteristics of sites 1 and 2 previously described by the 'five-point' model [3–6]. By increasing the

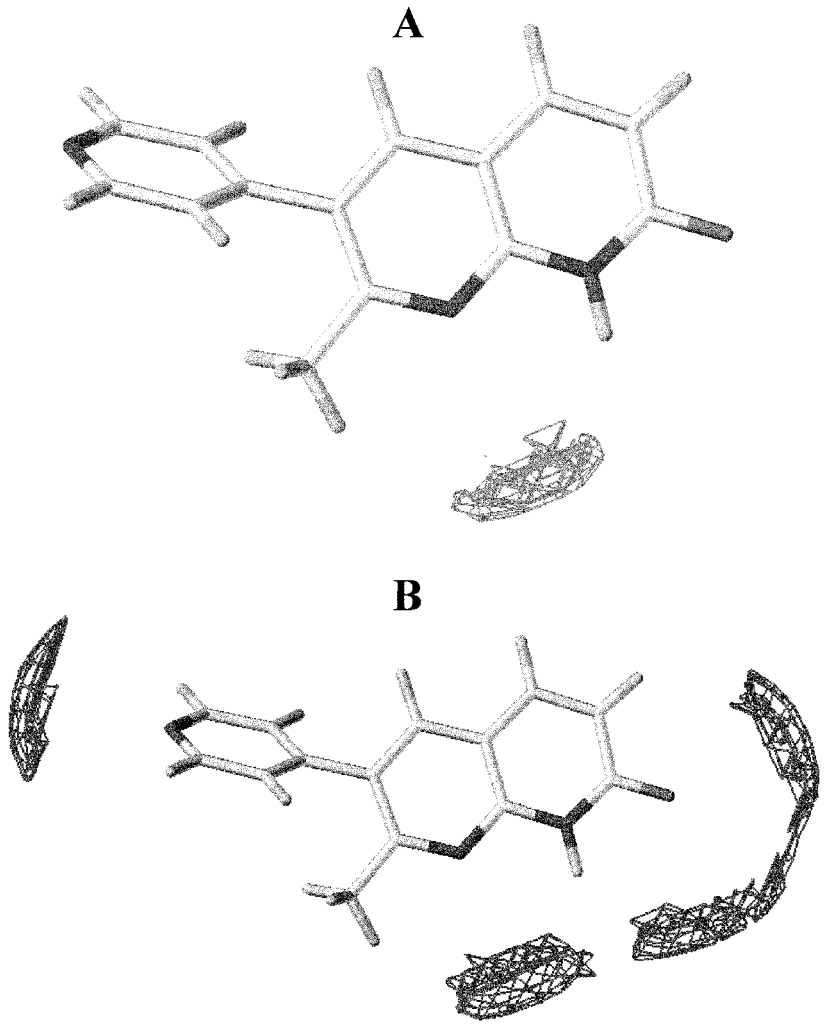

Figure 4. A: GRID energy contours (at −5.6 kcal/mol) indicating the most favourable binding site for the aliphatic hydroxyl probe and compound **6**. B: GRID energy contours (at −4.5 kcal/mol) indicating the three optimal areas of interaction for the aliphatic hydroxyl probe and compound **6**.

minimum input number of the required common site points, DISCO proposed two models, with the same number of pharmacophoric points, the same tolerance and the same sum of the energies of the conformers but different Dmean values. Model B, with lower Dmean value, was therefore chosen. It is an eight-point model (AL, DL, AS, HY, DS, DS, AL, DS), with tolerance of 2.50 Å (Figure 2), derived from compounds **1**, **3**, **5–11** and cAMP.

In addition to Model A, Model B contains the five features of Model A and adds a sixth feature, a hydrogen bond accepting site (AL) which corresponds to either a basic nitrogen atom (**1**, **3**, **5–7**, **9–11**, cAMP) or a carbonyl functional group (**8**), which represents the electron rich zone opposite to the primary site of binding already described in the latest topographical model of PDE III catalytic site proposed by Erhardt [6]. Interestingly, however, anagrelide **4** is discarded in this DISCO run even if it displays in this area an electron rich centre such as the chlorine atom at position 6. In fact this electron withdrawing atom is unable to make the requested interaction via an H-bond with the enzyme. The DISCO strategy would then suggest to take again into account the initially hypothesized feature the inhibitor should possess for the best interaction with the enzyme at this level, namely a hydrogen bond acceptor atom. Furthermore, examining the alignment of the cAMP molecule in Model B,

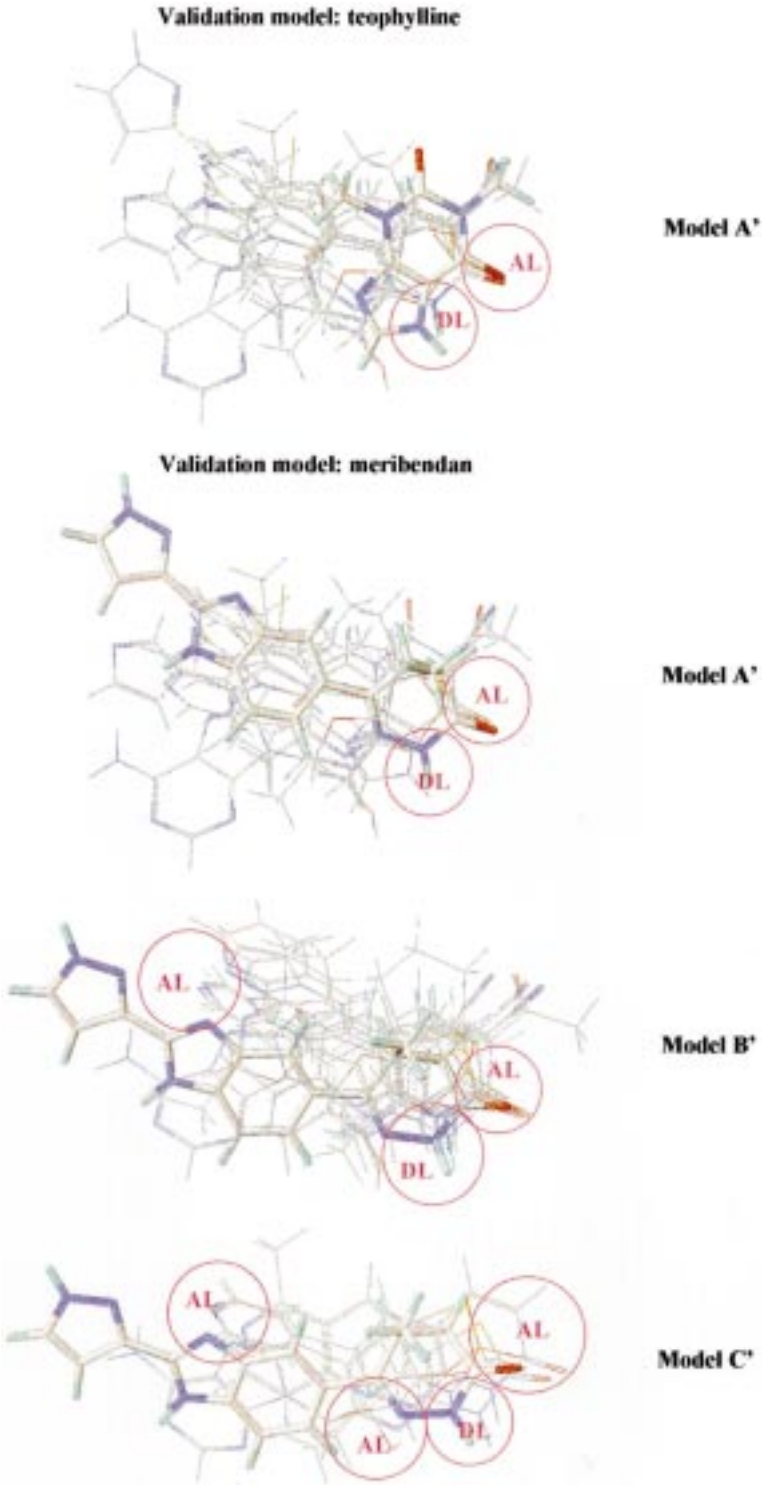

Figure 5. Validation model. From top to bottom: fitting of teophylline with Model A′, fitting of meribendan with Model A′, Model B′ and Model C′.

it seems that interaction with the biomolecule in this region involves nitrogen in position 7 of the adenosine ring instead of nitrogen in position 9 as previously assumed [4].

Lastly, an eleven point model (AL, DL, HY, DS, DS, HY, AL, AS, AL, HY, DS), Model C, with a distance tolerance of 2.50 Å was obtained by DISCO (Figure 2) keeping only compounds **5–7** plus cAMP. This model incorporates a new binding site, AL, a basic nitrogen which is consistent with recent findings by Singh et al. [18]. The marked difference in selectivity of compound **5** and analogues over that of milrinone **1** could in fact be explained by the presence of a basic nitrogen adjacent to the lactam moiety, which is able to strengthen the binding at the primary site via H-bonding or ionic interaction.

A rectangular box encompassing the 12 superimposed structures derived from the first DISCO model (Model A) was defined such that the box is extended beyond the molecular dimensions by 4.5 Å in all directions. GRID calculations were performed using 0.5 Å spacing between the grid points in this box, which measured 23 × 16 × 21 Å (for a total of 66693 grid points). For each target the non-bonded interaction energies with eight different probes were calculated using GRID. The probes used were: carboxylate group (CO_2^-), ammonium group (NH_3^+), sodium cation (Na^+), phenol hydroxyl group (*Ar*-OH), aliphatic hydroxyl group (*R*-OH), water, methyl group (CH_3), and the 'DRY' probe present in the program GRID. These probes may simulate negatively charged, positively charged, hydrogen-bonding donor/acceptor and hydrophobic-site residues respectively. These eight different probes were used in order to better explore which kind of amino acid residues interacting with the ligands are responsible for selectivity. In fact, at the moment, neither X-ray data of any PDE nor homology building studies on 3D models of PDEs catalytic site have been published yet. Only the primary sequence of PDE III is known, consequently, we are lacking information concerning which kind of amino acid residues in the PDE III catalytic site interact with ligands.

The interaction energies were calculated between each of the 12 ligands and 8 probes at each of the 66693 grid points.

A similar approach has been applied using the second DISCO superimposition (Model B). Here only 10 of the original 12 structures are evaluated. Since compound **4** has been discarded by the DISCO model because it displays a chlorine atom in position 6 instead of a hydrogen bond acceptor atom, it has been graphically included in the alignment in order to test the result provided by DISCO on this compound. GRID calculations were performed using 1 Å spacing between the grid points in a new common box which measured 23 × 22 × 21 Å (the larger value of grid spacing was due to the bigger dimensions of the box). The same eight probes previously described were used and eight new matrices, one for each probe, were obtained.

Principal Component Analysis (PCA) was consequently applied, for each probe separately, to reduce the number of original variables to a greatly reduced set of new variables, called Principal Components (PC). In this study for each probe the first five PCs explained about 70–80% of the total variance. Since the PCA has been performed on the column centred data matrices, we use the term eigenvectors instead of principal components.

The most interesting results were obtained using the first DISCO model (Model A) with the aliphatic hydroxyl probe and, in a similar way, with the phenol hydroxyl probe. According to recent site-directed mutagenesis experiments, a threonine residue (Thr^{349}) seems to be essential for PDE III catalytic activity [19], we therefore decided to present the results obtained with the aliphatic instead of the aromatic hydroxyl probe.

The score plot A reported in Figure 3 shows the two first eigenvectors for the aliphatic hydroxyl probe for Model A; the probe is able of donating and accepting one hydrogen bond. Four different groups of molecules are evident in this plot: cAMP; compounds **2**, **4**, **5**, **6**, **7**; compound **3**; compounds **1**, **8**, **9**, **10**, **11**.

The first group contains the natural endogenous substrate of the enzyme as unique member, the second group collects together the molecules displaying a basic nitrogen adjacent to the lactam moiety (**2**, **4**, **5**, **6**, **7**). These compounds are very selective inhibitors, however, among them compounds **2** and **4** are less selective than **5**, **6**, and **7**. The analysis of the score plot B, on the second vs. fifth eigenvectors (Figure 3), demonstrates that compounds **2** and **4** are separated from **5**, **6**, **7**. This feature is apparently a result of structural differences in the zone opposite to the primary site of the Erhardt model which determine a negative effect on the selectivity of the inhibitors: compound **2** in fact has its hydrogen acceptor site in this area too far removed for the optimal interaction with the enzyme, while compound **4** with a chlorine atom in this area has no possibility to form a hydrogen bond with the enzyme. The third group, reported in score plot A (Figure 3), contains only compound **3**, separated

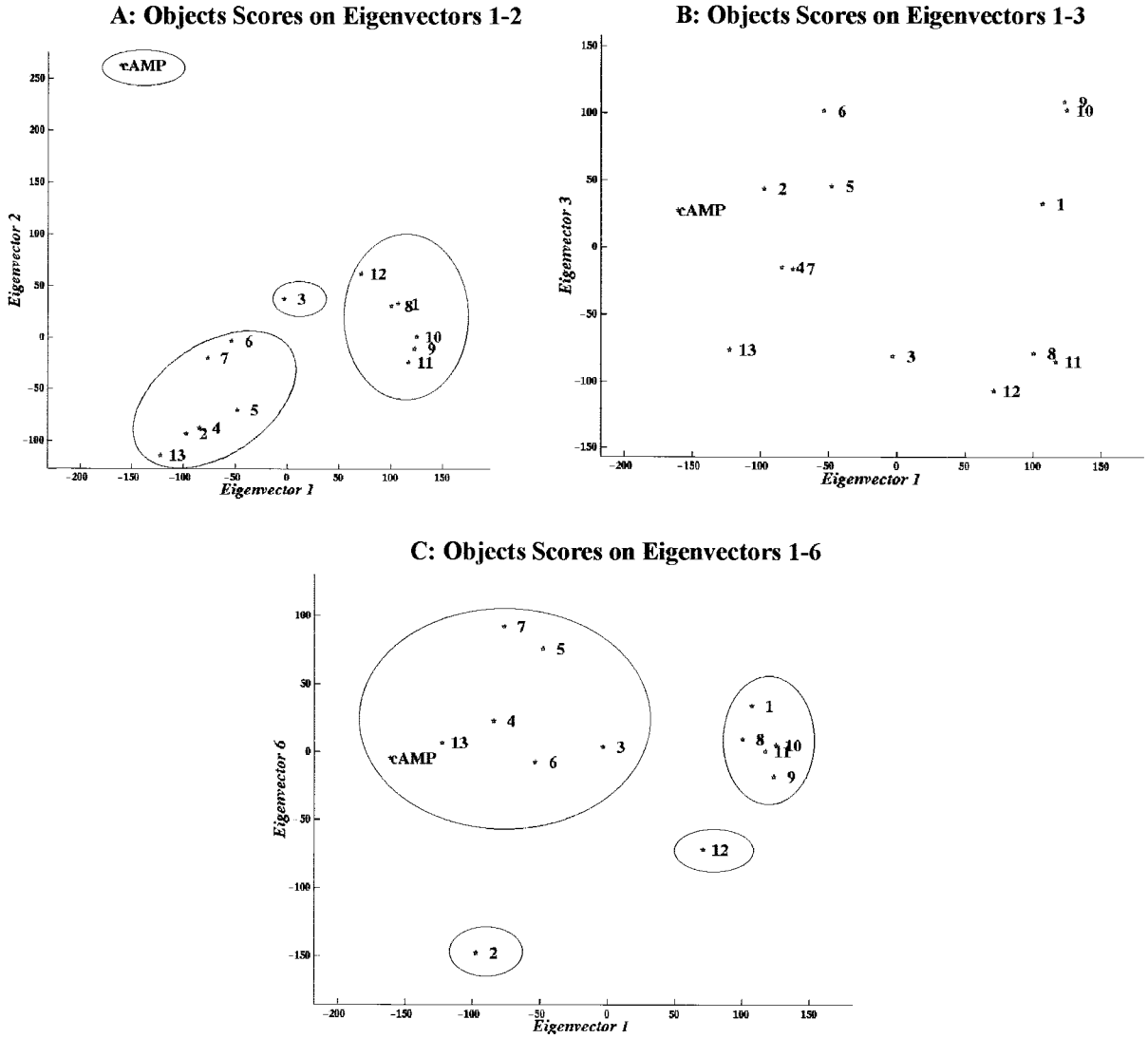

Figure 6. Validation model. A: Score plot of the first eigenvector vs. the second. This plot shows four separate groups of molecules indicated with circles. B: Score plot of the first eigenvector vs. the third. A selectivity trend from the bottom right to the top left of the plot is evident. C: Score plot of the first eigenvector vs. the sixth. Compound **2** is ungrouped from the most selective compounds on the sixth eigenvector.

from the others since it has neither the basic nitrogen atom near the lactam moiety nor a dipole, as a cyano or a carbonyl group, adjacent to the lactam moiety on the pyridone ring and this could probably account for its degree of selectivity towards the enzyme. The last group collects all the inhibitors lacking the extra basic nitrogen atom already described, but having the dipole adjacent to the lactam moiety. They are molecules with very different selectivity values. This fact may suggest the inability of the aliphatic hydroxyl probe to distinguish among them.

Observing the most favourable interactions between the aliphatic hydroxyl probe and the more potent and selective molecules (**5**, **6**, **7**) (GRID contour maps at −5.6 kcal/mol, Figure 4A), one can hypothesize that an *R*-OH amino acid residue could be able, at the same time, to accept the hydrogen of the lactam moiety and to donate its hydrogen to the basic nitrogen adjacent to the lactam moiety, making the interaction between the ligand and the enzyme more stable. Therefore the important role of this basic nitrogen is again proved, suggesting an important structural modification that should be applied to our compounds.

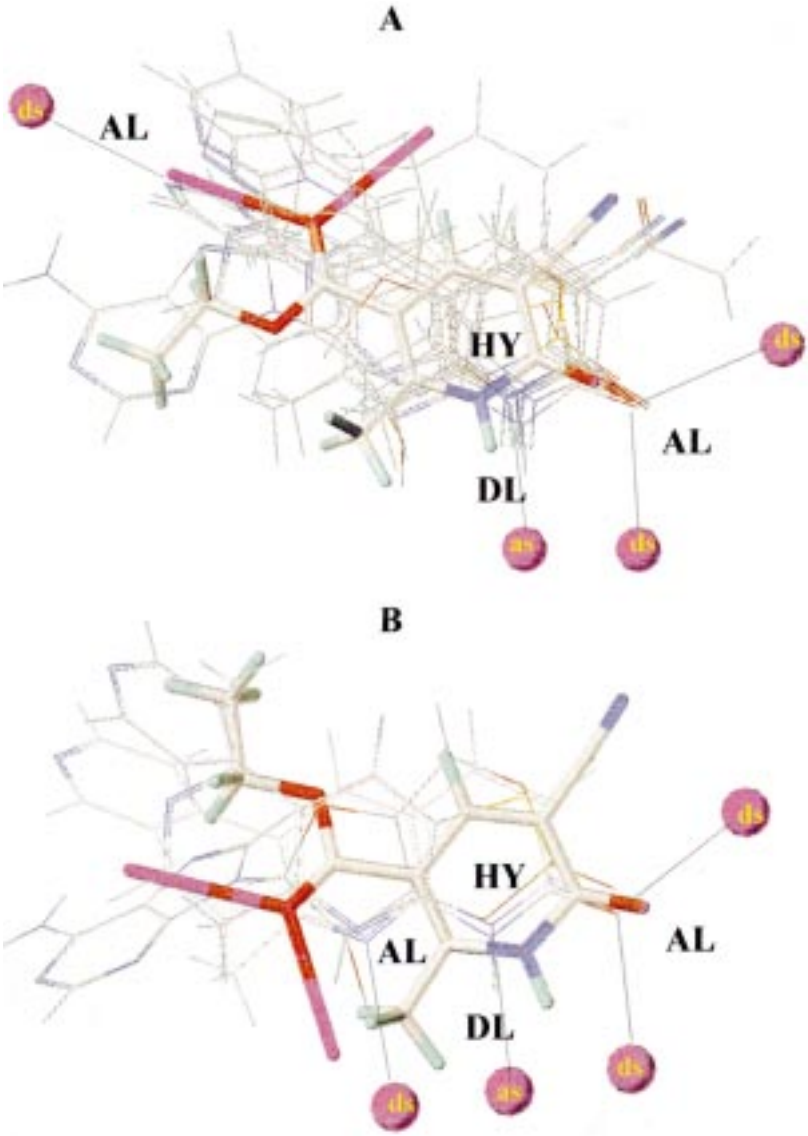

Figure 7. A: Fitting of compound **8** with Model B. B: Fitting of compound **8** with Model C.

The GRID contour maps at −4.5 kcal/mol (Figure 4B) confirm the presence of three main binding areas as proposed by the last DISCO model (Model C).

These results, obtained using the simplest DISCO model (Model A) as starting point, confirm the ones derived from the other DISCO models (Models B and C) and provide a computational strategy to predict the selectivity of new ligands. One can in fact rationally design a new molecule or modify a previous one, align it to a set of selective inhibitors using DISCO and calculate the grid energies with the *R*-OH probe, then verify its position on the scores plot.

The results obtained with the other probes only in some cases confirm the *R*-OH results and do not give any additional useful information. Similar conclusions were obtained with the second DISCO superimposition (Model B).

The derived pharmacophoric model was validated in its capability of distinguishing between selective and non-selective inhibitors, testing teophylline **12** [20], and meribendan **13** [21], a non-selective and selective inhibitor of the enzyme respectively.

The validation was performed adding teophylline and meribendan to the set of molecules previously

taken into account (training set). We asked DISCO to derive Model A′, Model B′ and Model C′, with exactly the same features as Model A, Model B and Model C, respectively.

As expected, teophylline fits only Model A′ (Figure 5) and it is confirmed as a non-selective agent. Probably, the features of Model A (or A′) are essential, but not sufficient for selective inhibition of PDE III.

On the contrary, meribendan, a very selective inhibitor, fits well all the three models (Figure 5). It displays a higher level of selectivity in comparison with the parent compound **2** because, beside the basic nitrogen adjacent to the lactam moiety (necessary for fitting Model C) it possesses another basic nitrogen (benzimidazole ring), opposite to the primary binding site, located in the right position for fitting Model B.

The 3D-SAR (GRID plus PCA) was subsequently performed on the 14 aligned structures of Model A′.

The results were in agreement with those obtained with the training set and confirmed teophylline and meribendan as a non-selective and a very selective inhibitor respectively. The first six PCs explained about 80% of the total variance.

The score plot A reported in Figure 6 shows the two first eigenvectors and it has the same pattern described in Figure 3. In the score plot B, on the first vs. third eigenvectors (Figure 6) is evident an 'increasing selectivity direction' from the bottom right to the top left of the plot. The less selective compounds (**8**, **11**, **12**) are followed by the others according to an increase of enzymatic selectivity. Compound **2** is an exception to this trend, but it is separated from the most selective structures on the sixth eigenvector (Figure 6, score plot C) while compound **13** is always correctly grouped with the most selective inhibitors.

Conclusions

Two principal conclusions may be drawn from this study.

First, the synergistic combination of DISCO, GRID and PCA strategies may be proposed as a useful tool in the rational approach to drug design and second, when the biological activities can be considered quantitatively (and not only qualitatively, as in the present work), one could apply this strategy for a QSAR study using the PLS regression method to predict the biological activity of new compounds.

In addition, the pharmacophoric model described here defines in greater detail the structural requirements necessary for potent and selective inhibition of PDE III, and suggests ways of further increasing the potency and the selectivity of these inhibitors. Compound **8** in fact is able to reach the second region of binding described in Model B (Figure 7A) but only in alternative reaches the extra binding site shown in Model C (Figure 7B), thanks to one of the lone pairs of the carbonyl function.

The reason for its lower selectivity towards the enzyme in comparison with **5** or **7** could consequently be explained through the inability of the molecule of interacting simultaneously with the second hydrogen bonding zone of Model B and the extra binding site of Model C.

The synthesis of a conformationally constrained analogue of **8**, possessing both the carbonyl group and an extra nitrogen adjacent to the primary site of binding, will be a further development of the present work.

Acknowledgements

The Italian funding agencies of MURST and CNR are gratefully acknowledged for financial support.

References

1. Alousi, A.A., Canter, J.M., Montenaro, M.J., Fort, D.J. and Ferrari, R.A., J. Cardiovasc. Pharmacol., 5 (1983) 792.
2. Butt, E., Beltman, J., Becker, D.E., Jensen, G.S., Rybalkih, S.D., Jastorff, B. and Beavo, J.A., Mol. Pharmacol., 47 (1995) 340.
3. Bristol, J.A., Sircar, I., Moos, W.H., Evans, D.B. and Weishaar, R.E., J. Med. Chem., 27 (1984) 1099.
4. Erhardt, P.W., Hagedorn III, A.A. and Sabio, M., Mol. Pharmacol., 33 (1988) 1.
5. Moos, W.H., Humblet, C.C., Sircar, I., Rithner, C., Weishaar, R.E., Bristol, J.A. and McPhail, A.T., J. Med. Chem., 30 (1987) 1963.
6. Erhardt, P.W. and Chou, Y.L., Life Sci., 49 (1991) 553.
7. Mosti, L., Menozzi, G., Schenone, P., Dorigo, P., Gaion, R.M., Benetollo, F. and Bombieri, G., Eur. J. Med. Chem., 24 (1989) 517.
8. Martin, Y.C., Bures, M.G., Danaher, E.A., De Lazzer, J., Lico, I. and Pavlik, P.A., J. Comput.-Aided Mol. Design, 7 (1993) 83.
9. Sybyl, Version 6.2, Tripos Inc., St. Louis, MO, 1995.
10. Goodford, P., J. Chemometrics, 10 (1996) 107.
11. Manly, B.F., Multivariate Statistical Methods – A Primer, Chapman and Hall, London, 1989.
12. MacroModel, Version 5.5, Columbia University, New York, NY, 1996.
13. Mohamadi, F., Richards, N.G.J., Guida, W.C., Liskamp, R., Caufield, C., Chang, G., Hendrickson, T. and Still, W.C., J. Comput.-Aided Mol. Design, 4 (1990) 440.

14. Gundertofte, K., Liljefors, T., Norrby, P.O. and Pettersson, I., J. Comput. Chem., 17 (1996) 429.
15. Apaya, R.P., Lucchese, B., Price, S.L. and Vinter, J.G., J. Comput.-Aided Mol. Design, 9 (1995) 33.
16. Fossa, P., Altomare, C., Cellamare, S., Summo, L., Mosti, L. and Carotti, A., Acta First Italian–Swiss Meeting Med. Chem., (1997) 128.
17. Allen, F.H., Bellard, S., Brice, M.D., Cartwright, B.A., Doubleday, A., Higgs, H., Hummelink, T., Hummelink-Peters, B.G., Kennard, O., Motherwell, W.D.S., Rodgers, J.R. and Watson, D.G., Acta Crystallogr., B35 (1979) 2331.
18. Singh, B., Bacon, E.R., Lesher, G.Y., Robinson, S., Pennock, P.O., Bode, D.C., Pagani, E.D., Bentley, R.G., Connell, M.J., Hamel, L.T. and Silver, P.J., J. Med. Chem., 38 (1995) 2546.
19. Jin, S.L.C., Swinnen, J.V. and Conti, M., J. Biol. Chem., 267 (1992) 18929.
20. Schudt, C., Winder, S., Müller, B. and Ukena, D., Biochem. Pharmacol., 42 (1991) 153.
21. Jonas, R., Klockow, M., Lues, I., Prücher, H., Schliep, H.J. and Wurziger, H., Eur. J. Med. Chem., 28 (1993) 129.
22. Singh, B., Lesher, G.Y., Pluncket, K.C., Pagani, E.D., Bode, D.C., Bentley, R.G., Connell, M.J., Hamel, L.T. and Silver, P.J., J. Med. Chem., 35 (1992) 4858.
23. Singh, B., Bacon, E.R., Robinson, S., Fritz, R.K., Lesher, G.Y., Kumar, V., Dority, J.A., Reuman, M., Kuo, G.H., Eissenstat, M.A., Pagani, E.D., Bode, D.C., Bentley, R.G., Connell, M.J., Hamel, L.T. and Silver, P.J., J. Med. Chem., 37 (1994) 248.
24. U.S. Patent 5141931, Annu. Drug Data Report, 17 (1995) 256.
25. Sugioka, M., Ito, M., Masuoka, H., Ichikawa, K., Konishi, T., Tanaka, T. and Nakano, T., Naunyn-Schmiedeberg's Arch. Pharmacol., 350 (1994) 284.